The Chemist
Journal of the American Institute of Chemists

Phase Equilibria in the Tl_2Te-Tl_5Te_3-Tl_9SmTe_6 System

Samira Zakir Imamaliyeva*, Vagif Akber Gasymov, Mahammad Baba Babanly
Institute of Catalysis and Inorganic Chemistry named after acad. M. Nagiyev
National Academy of Science of Azerbaijan, H. Javid Ave., 131, Az-1143, Baku, Azerbaijan
*(*E-mail: samira9597a@gmail.com)*

Abstract: Phase equilibria in the Tl_2Te-Tl_5Te_3-Tl_9SmTe_6 system were experimentally studied by means of differential thermal analysis, powder X-ray diffraction technique and microhardness measurements applied to equilibrated alloys. Several isopleth sections and isothermal section at 300 K, as well as projections of the liquidus and solidus surfaces, were constructed based on the experimental data. It was established that homogeneity area of solid solutions with Tl_5Te_3 structure (δ-phase) occupied more than 90% of the concentration triangle. A narrow area of solid solutions (α-phase) based on Tl_2Te was detected.

Key Words: thallium-samarium tellurides, phase equilibria, solid solutions, crystal structure.

INTRODUCTION

Chalcogenides of heavy p-elements have received a lot of attention thanks to their interesting functional properties, such as thermoelectric, photoelectric, optical, magnetic properties [1-3]. Furthermore, in recent years some of such compounds have attracted both scientific and technological interest as topological insulators [4-6]. Doping by rare-earth elements can improve their properties and give them additional functionality, such as the magnetic properties [7,8].

Thallium subtelluride, Tl_5Te_3 is suitable "matrix" for creation of new complex materials. This compound crystallizes in tetragonal structure [9] (Sp.gr.I4/mcm) with four formula units per unit cell (Fig.1). The basic structural component of Tl_5Te_3 compound is octahedron with a thallium atom, Tl(2), in its center. These octahedra connected by vertices form a frame Tl_4Te_{12}, or $(TlTe_3)_4$. The other 16 thallium atoms, Tl(1) link octahedra along the *c* axis and form a unit cell $Tl_{16}(TlTe_3)_4$. B^{3+} (B^{3+}-Sb, Bi) substitution for half of the Tl(2) atoms, resulting in the compounds Tl_9BTe_6 or $Tl_{16}[(Tl^{1+}_{0,5}B^{3+}_{0,5})Te_3]_4$ (I), while the replacement of all these thallium atoms by cations A^{2+} (A^{2+}-Sn, Pb) leading to formation of Tl_4ATe_3 or $Tl_{16}[A^{2+}Te_3]_4$ (II).

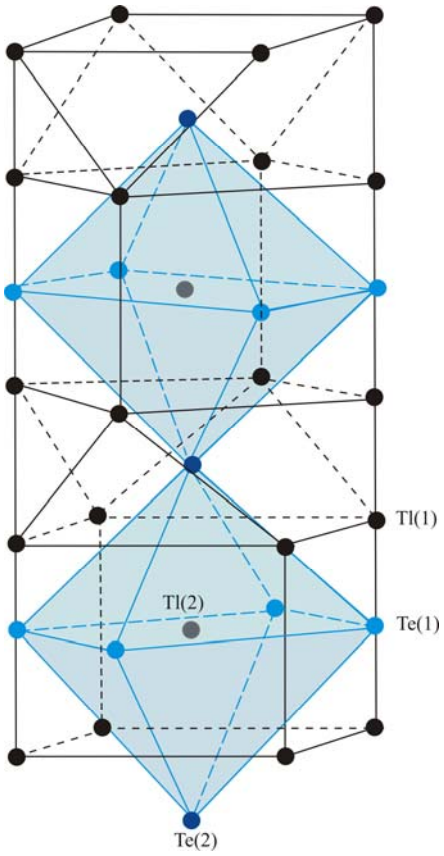

Fig 1. Basic structural component of Tl_5Te_3 compound.

Compounds of type (I) and (II) were detected during the experimental phase equilibria studies of respective ternary systems [10-13]. These materials possess thermoelectric properties, and Tl_9BiTe_6 was found to have the highest ZT value [1,2,14].

A new thallium lanthanide tellurides with composition Tl_9LnTe_6 (Ln-Ce, Nd, Sm, Gd, Tm, Tb) were obtained first by Babanly M.B. [15-17]. It was shown that above mentioned compounds are substitution variants of Tl_5Te_3, and their melting character and crystal lattices parameters were determined. Moreover, ytterbium does not form the compound Tl_9YbTe_6 [17, 18]. Later, the crystal structure as well as magnetic and thermoelectric properties for a number Tl_9LnT_6-type compounds were determined by authors [19-21].

According to the phase diagrams [10-13, 15], all listed ternary compounds are phases with variable composition and have wide homogeneity areas.

In our previous papers [22-25], we have presented the results of phase equilibria investigations of the Tl_5Te_3-Tl_9NdTe_6-Tl_9BiTe_6, Tl_5Te_3-Tl_4PbTe_3-Tl_9NdTe_6, Tl_9NdTe_6-Tl_9BiTe_6-Tl_4PbTe_3, Tl_2Te-Tl_9NdTe_6-Tl_9BiTe_6, and Tl_2Te-Tl_9TbTe_6 systems including Tl_5Te_3 compound or its structural analogues. We found that the former three systems are characterized by formation of continuous solid solutions and the latter two systems- by wide areas of solid solutions.

Here we represent a detailed investigation of phase relationships of the Tl-Sm-Te system in the Tl_2Te-Tl_5Te_3-Tl_9SmTe_6 composition area.

Tl_2Te and Tl_5Te_3 compounds melt congruently at 698 and 723 K and form the eutectic (695 K, ~ 34 at.% Tl) [26]. These data were confirmed by Okamoto [27]. Tl_2Te crystallizes in the monoclinic system (space group C2/c; a = 15.662; b = 8.987; c=31.196 Å, β=100.76^0, z=44) [28], while tetragonal lattice parameters of Tl_5Te_3 are equal to a = 8.930; c = 12.598 Å [9]. Tl_9SmTe_6 melts with decomposition by the peritectic reaction at 755 K and has lattice constant: a=8.888; c=13.013 Å, z=2 [16].

EXPERIMENTAL

Materials and Syntheses

Starting compounds Tl_2Te and Tl_5Te_3 were synthesized by melting of high purity elements in evacuated (~ 10^{-2} Pa) quartz ampoules at 750 K with following slow cooling. Tl_9SmTe_6 was synthesized at 1000 K using the ceramic method. Taking into account the incongruent melting of Tl_9SmTe_6 [16], this compound was annealed at 700 K for 300 h after the synthesis.

The purity of the synthesized compounds was checked by differential thermal analysis (DTA) and powder X-ray diffraction (XRD) techniques.

Alloys of the Tl_2Te-Tl_5Te_3-Tl_9SmTe_6 system were prepared by melting the stoichiometric quantities of the pre-synthesized binary and ternary compounds in evacuated silica ampoules at 900 K in a tube furnace. After the synthesis, alloys were powdered in an agate mortar, pressed into pellets and reheated at 680 K within 1000 h. In order to prevent a reaction between the ampoules and samarium, the silica tubes were coated with a carbon film via the decomposition of ethanol.

Methods

DTA and XRD analyses as well as microhardness measurements were employed to analyze the samples.

DTA was performed using a NETZSCH 404 F1 Pegasus differential scanning calorimeter. The crystal structure was analyzed by a powder X-ray diffraction technique at room temperature using a Bruker D8 diffractometer utilizing CuK_α radiation within 2θ = 10 to 70°. Microhardness measurements were done with a microhardness tester PMT-3, the typical loading being 20g.

RESULTS & DISCUSSION

The combined analysis of experimental data enabled us to construct the self-consistent diagram of the phase equilibria in the Tl_2Te-Tl_5Te_3-Tl_9SmTe_6 system (Table, Fig.2-7).

The (16/3)**Tl_2Te-Tl_9SmTe_6** system (Fig.2) is a part of the Tl_2Te-Sm_2Te_3 system. It is a non-quasi-binary because of the incongruent character of the Tl_9SmTe_6 melting. However, it behaves as a quasi-binary system below the peritectic horizontal at 755 K. The phase diagram is characterized by formation of a wide area of solid solutions (δ) with the Tl_5Te_3 structure. Liquidus consists of three curves corresponding to the primary crystallization of α- and δ- phases based on Tl_2Te and Tl_9SmTe_6, as well as the unknown infusible X phase (presumably $TlSmTe_2$). Horizontals at 755 and 703 K correspond to peritectic equilibria $L+X \leftrightarrow \delta$ and $L+\delta \leftrightarrow \alpha$. The peritectic points p_1 and p_2 correspond to 65 and 5 mol% Tl_9SmTe_6, respectively.

The equilibrium phase diagram of the **$2Tl_5Te_3$-Tl_9SmTe_6** system (Fig.3) is also non-quasi-binary due to

peritectic melting of Tl_9SmTe_6 compound. This system is characterized by the formation of a continuous series of solid solutions (δ) based on Tl_5Te_3. The δ-solid solutions primarily crystallize in 0-65 mol% Tl_9SmTe_6 composition area; whereas in region more than 65 mol% Tl_9SmTe_6, the X phase crystallizes. In this composition area below 755 K, a three-phase area L+X+δ should be formed as the result of monovariant peritectic reaction L+X↔δ. However, this area is not experimentally fixed due to narrow temperature interval and shown by dashed line (Fig.3a).

Table 1. Some properties of phases in the Tl_2Te-Tl_5Te_3-Tl_9SmTe_6 system.

System	Phase	Thermal effects, K	Sp.gr	Lattice parameters, Å	H_μ, MPa
	Tl_2Te	698	monoclinic, *C2/c*;	*a* = 15.662; *b* = 8.987; *c* = 31.196Å, β = 100.760, z = 44	1400
	Tl_5Te_3	723	tetragonal, I4/mcm	*a*=8.930; *c*=12.598	1130
	Tl_9SmTe_6	755; 1180	"-"	*a*=8.888; *c*=13.013	1080
$2Tl_5Te_3$-Tl_9SmTe_6	$Tl_{9.8}Sm_{0.2}Te_6$	725-733	"-"	*a*=8.922; *c*=12.681	1130
	$Tl_{9.6}Sm_{0.4}Te_6$	730-740	"-"	*a*=8.913; *c*=12.764	1170
	$Tl_{9.5}Sm_{0.5}Te_6$	735-743	-		
	$Tl_{9.4}Sm_{0.6}Te_6$	735-745	"-"	*a*=8.905; *c*=12.847	1150
	$Tl_{9.2}Sm_{0.8}Te_6$	742-750; 1110	"-"	*a*=8.896; *c*=12.930	1120
$\frac{16}{3}Tl_2Te$-Tl_9SmTe_6	$Tl_{9.8}Sm_{0.2}Te_{5,2}$	703-728	"-"	-	1240; 1480
	$Tl_{9.6}Sm_{0.4}Te_{5,4}$	713-747	"-"	*a*=8.912; *c*=12.782	1200
	$Tl_{9.6}Sm_{0.5}Te_{5,5}$	723-752	-		
	$Tl_{9.4}Sm_{0.6}Te_{5,6}$	733-755	"-"	*a*=8.903; *c*=12.864	1190
	$Tl_{9.2}Sm_{0.8}Te_{5,8}$	742-755; 1112	"-"	*a*=8.894; *c*=12.955	1150

The results of the microhardness measurements are in agreement with constructed phase diagram (Figs.2b and 3b). For the Tl_5Te_3-Tl_9SmTe_6 system, a curve has a flat maximum (Fig.3b), which is typical for systems with continuous solid solutions. For the Tl_2Te-Tl_9SmTe_6 system, the microhardness values of starting compounds are increased within homogeneity areas of α- and δ-phases, and remain constant in the α+δ two-phase region (Fig.2b).

Powder X-ray analysis data confirm the phase diagrams of the above-mentioned systems (Fig.4). For the Tl_5Te_3-Tl_9SmTe_6 system, powder diffraction patterns of starting compounds and intermediate alloys are qualitatively similar with slight reflections displacement from one compound to another (Fig.4, diffraction patterns 4-6). For example, we present the powder diffraction pattern of alloy with 50 mol% Tl_9SmTe_6. Solid solutions obey the Vegard's law, i.e. the lattice parameters depend linearly on composition. In the Tl_2Te-Tl_9SmTe_6 system, the alloys with compositions ≥30 mol% Tl_9SmTe_6 are monophasic with Tl_5Te_3-type diffraction patterns (Fig.4, diffraction pattern 3), while alloy with 25mol% Tl_9SmTe_6

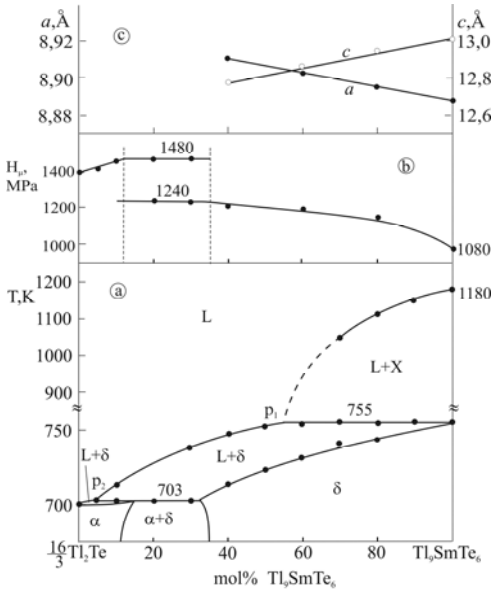

Fig 2. Phase diagram (a), concentration relations of microhardnesses (b), and lattice parameters (c) for the system (16/3)Tl_2Te-Tl_9SmTe_6.

composition is bi-phasic. Besides the δ-phase reflections this alloy contains weak peaks of α-phase (Fig.4, diffraction pattern 2).

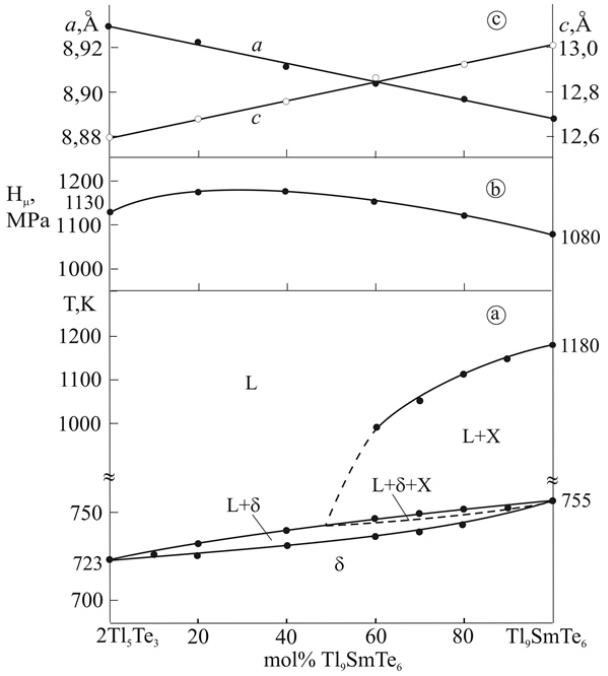

Fig 3. Phase diagram (a), concentration relations of microhardnesses (b), and lattice parameters (c) for the system $2Tl_5Te_3$-Tl_9SmTe_6.

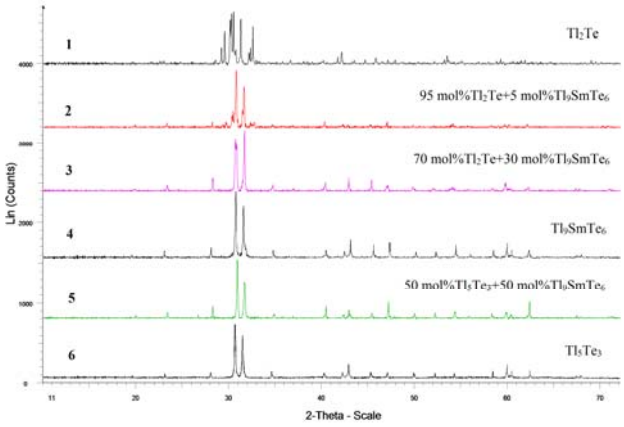

Fig 4. XRD patterns for different compositions in the Tl_2Te-Tl_9SmTe_6 (patterns 1-4) and Tl_5Te_3-Tl_9SmTe_6 (patterns 4-6) systems.

Isopleth sections of the Tl_2Te-Tl_5Te_3-Tl_9SmTe_6 system (Fig.5).

Figs. 5a-c show the isopleth sections Tl_5Te_3-[A], Tl_9SmTe_6-[B] and Tl_2Te-[C] of the Tl_2Te-Tl_5Te_3-Tl_9SmTe_6 system, where A, B and C are alloys from the respective boundary system. As can be seen, over the entire compositions range of the Tl_5Te_3-[A] system only δ-phase crystallizes from the melt.

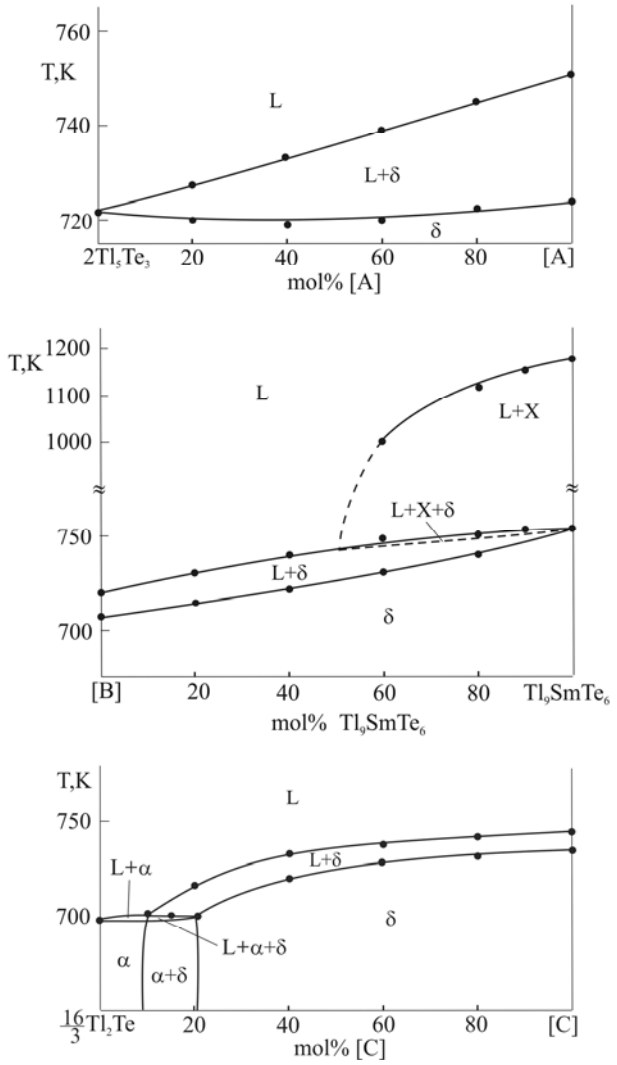

Fig 5. Polythermal sections $2Tl_5Te_3$-[A], Tl_9SmTe_6-[B] and (16/3)Tl_2Te-[C] of the phase diagram of the Tl_2Te-Tl_5Te_3-Tl_9SmTe_6 system.

According to the phase diagram of the Tl_9SmTe_6-[B] section in the composition area <50 mol% Tl_9SmTe_6, the primary crystallization of the δ-phase occurs from the liquid phase. In the Tl_9SmTe_6- rich alloys the X-phase first crystallizes, then a monovariant peritectic equilibrium L+X↔δ takes place.

The liquidus of Tl_2Te-[C] section consists of two curves of primary crystallization of α- and δ-phases. The intersection point of these curves corresponds to the monovariant peritectic reaction L+δ↔α (703 K). Below the solidus, this section passes through the α, α+δ and δ phase areas.

The isothermal sections of the Tl_2Te-Tl_5Te_3-Tl_9SmTe_6 system at 300 K (Fig.6)

The isothermal sections of the Tl_2Te-Tl_5Te_3-Tl_9SmTe_6 system at 300 K (Fig.6) consists of three phase areas. Over 90% of the concentration triangle is occupied by δ-solid solutions with Tl_5Te_3 structure. α-phase based on Tl_2Te has a narrow homogeneity area in the corresponding angle of the triangle. Homogeneity areas of the α- and δ-phases are separated by α+δ two-phase region.

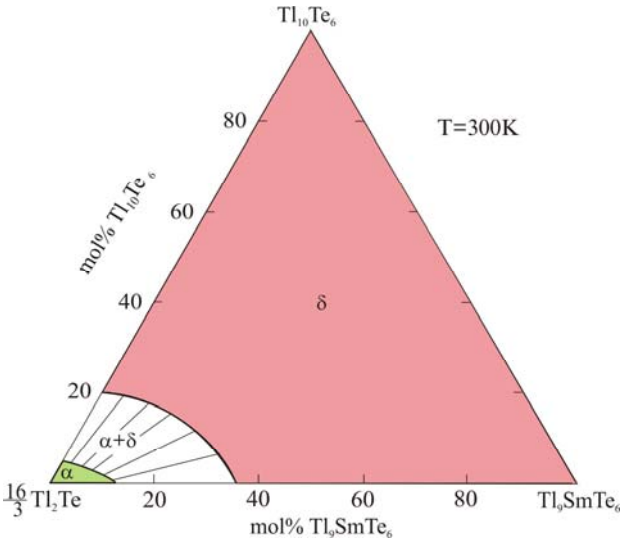

Fig 6. Isothermal section of the phase diagram of the Tl_2Te-Tl_5Te_3-Tl_9SmTe_6 system at 300 K.

The liquidus surface projection (Fig.7)

Liquidus of Tl_2Te-Tl_5Te_3-Tl_9SmTe_6 system consists of three fields of the primary crystallization of α-, δ- and X-phases. These fields are separated by p_2e and p_1p_1' lines, which correspond to the monovariant peritectic equilibria L+δ↔α and L+X↔δ. Near the eutectic point (e) the peritectic equilibrium L+δ↔α must be transformed into L↔α+δ eutectic equilibrium. However, coordinates of this transformation are not experimentally fixed due to narrow temperature range. Solidus surface consists of two areas corresponding to the completion of crystallization α- and δ-phases.

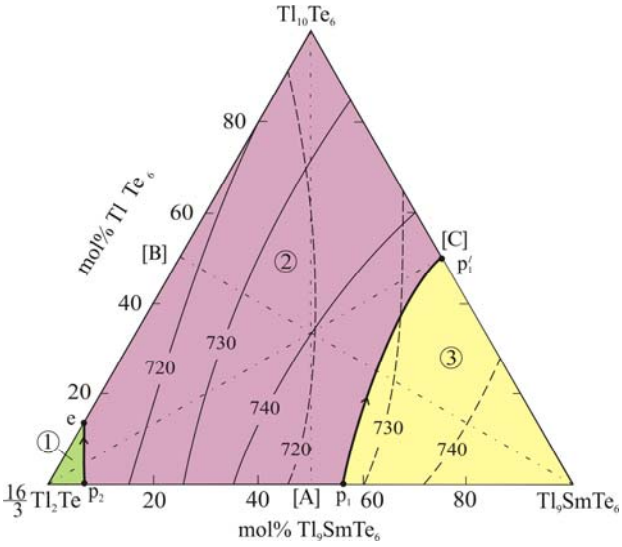

Fig 7. Projection of the liquidus and solidus (dashed lines) surfaces of the Tl_2Te-Tl_5Te_3-Tl_9SmTe_6 system. Primary crystallization fields of phases: 1-α; 2-δ; 3-X. Dash-dot lines show the investigated sections.

CONCLUSION

A complete T-x-y diagram of the Tl_2Te-Tl_5Te_3-Tl_9SmTe_6 system is constructed, including the T-x diagrams of boundary systems Tl_5Te_3-Tl_9SmTe_6 and Tl_2Te-Tl_9SmTe_6, some isopleth sections, isothermal section at 300 K and liquidus and solidus surface projections. Studied system is characterized by the formation of wide field of δ-solid solutions with the Tl_5Te_3 structure, occupying more than 90% of the concentration triangle. Obtained experimental data can be used for choosing the composition of solution-melt and for determining of temperature conditions for growing crystals of δ- phase with a given composition.

ACKNOWLEDGMENT

The work was supported by the Science Foundation of the State Oil Company of Azerbaijan Republic (Grant for the project "Preparation and investigation of new functional materials based on complex metal chalcogenides for alternative energy sources and electronic engineering", 2014).

REFERENCES

1. Shevelkov AV. *Russ. Chem. Rev*, 2008, 77, 1.
2. *CRC Handbook of Thermoelectrics*, ed. by D. M. Rowe. CRC Press, New York, 1995, 701p.
3. Koc H, Simsek S, Mamedov AM & Ozbay E. *Ferroelectrics*, 2015, 483(1), 43.
4. Niesner D, Otto S, Hermann V, Fauster Th, Menshchikova TV, Eremeev SV, Aliev ZS, Amiraslanov IR, Echenique PM, Babanly MB, Chulkov EV. *Phys.Rev.B*, 2014, 89, 081404.
5. Politano A, Caputo M, Nappini S, Bondino F, Aliev ZS, Babanly MB, Chulkov EV. *J.Phys.Chem*.C, 2014, 118, 21517.
6. Yan B, Zhang H-J, Liu C-X, Qi X-L, Frauenheim T and Zhang S-C. *Phys. Rev.B*, 2010, 82, 161108(R).
7. Alemi A, Klein A, Meyer G, Dolatyari M and Babalou AZ. *Anorg. Chem*, 2011, 637, 87.
8. Wu F, Song H, Jia J, Xu H. *Prog.Nat.Sci*, 2013, 23 (4), 408.
9. Schewe I, Böttcher P, Schnering HG. *Z.Kristallogr*, 1989, Bd188, 287.
10. Babanly MB, Akhmad'ar A, Kuliev AA. *Russ. J. Inorg. Chem*, 1985, 30, 1051.
11. Babanly MB, Akhmad'yar A, Kuliev AA. *Russ.J.Inorg. Chem*, 1985, 30, 2356.
12. Babanly MB, Gotuk A A, Kuliev AA. *Inorg.Mater*, 1979, 15, 1011.
13. Gotuk AA, Babanly M B, Kuliev AA. *Inorg. Mater*, 1979, 15, 1062.
14. Wolfing B, Kloc C, Teubner J, Bucher E. *Phys. Rev. Let*, 2001, 36 (19), 4350.
15. Imamaliyeva SZ, Sadygov FM, Babanly MB. *Inorg.Mater*, 2008, 44, 935.
16. Babanly MB, Imamaliyeva SZ, Babanly DM. *Azerb.Chem.J*, 2009, 2, 121.
17. Babanly MB, Imamaliyeva SZ, Sadygov FM. *News of BSU. Nat. Sci.Ser*, 2009, 4, 5.
18. Imamaliyeva SZ, Mashadiyeva LF, Zlomanov VP, Babanly MB. *Inorg.Mater*, 2015, 51, 1237.
19. Bangarigadu-Sanasy S, Sankar C R, Assoud A, Kleinke H. *Dalton Trans*, 2011, 40, 86.
20. Bangarigadu-Sanasy S, Sankar C R, Schlender P, Kleinke H. *J. Alloys Compd*, 2013, 549, 126.
21. Bangarigadu-Sanasy S, Sankar CR, Dube PA, Greedan JE, Kleinke H. *J.Alloys. Compd*, 589, (2014) 389.
22. Babanly MB, Tedenac J-C., Imamaliyeva SZ, Guseynov FN, Dashdieva GB. *J.Alloys Compd*, 2010, 491, 230.
23. Imamaliyeva SZ, Guseynov FN, Babanly MB. *J. Chem. Probl*, 2008, 4, 640.
24. Imamaliyeva SZ, Guseynov FN, Babanly M. *Azerb.Chem.J*, 2009, 1, 49.
25. Imamaliyeva SZ, Gasanly TM, Sadygov FM, Babanly MB. *Azerb.Chem.J*, 2015, 3, 93.
26. Asadov MM, Babanly MB, Kuliev AA. *Inorg. Mater*, 1977, 13(8), 1407.
27. Okamoto H. *J. Phase Equilib*, 2001, 21(5), 501.
28. Cerny R, Joubert J, Filinchuk Y, Feutelais Y. *Acta Crystallogr. C*, 2002, 58(5), 163.